Omnidirectional band gap in Fibonacci photonic crystals with metamaterials using a band-edge formalism

W. J. Hsueh,* C. T. Chen, and C. H. Chen
Department of Engineering Science, National Taiwan University, 1, Sec. 4, Roosevelt Road, Taipei, 10660, Taiwan
(Received 29 February 2008; published 24 July 2008)

Omnidirectional zero-$\bar{n}$ gaps in one-dimensional photonic crystals with a Fibonacci basis containing frequency dependent metamaterials are examined. In this study, the band structure and band gaps are determined by an explicit band-edge equation rather than by a traditional dispersion equation. We find that the present method has better numerical stability than traditional methods, especially for calculating the zero-$\bar{n}$ gap in the photonic crystals with metamaterials. We observe that the change in the width and location of the omnidirectional zero-$\bar{n}$ gap is limited for the Fibonacci photonic crystals with different generation orders. However, the width of the omnidirectional gap in the Fibonacci photonic crystals is significantly affected by the filling factor of the metamaterials. We also find that the width of the gap will be maximum at an optimum filling factor. The gap will vanish if the filling factor is greater than a critical value. Moreover, for a given filling factor and a metamaterial, it is interesting that the gap will be enlarged as the refractive index of the traditional layer increases.

DOI: 10.1103/PhysRevA.78.013836 PACS number(s): 42.70.Qs, 41.20.Jb, 78.20.Ci, 42.82.Et

I. INTRODUCTION

Metamaterials and left-handed materials have received much attention during the last few years. Although natural materials with negative permeability and permittivity have not been found, artificially composite materials made by periodical array of metallic split ring resonators and wires have been shown to have effective negative permeability and permittivity, simultaneously [1–9]. Due to the unusual properties of the metamaterials, optical wave propagating in one-dimensional (1D) photonic crystals consisting of metamaterials and conventional right-hand material layers have different results from conventional photonic crystals. For periodical structures, the band gaps and band structure are fundamental to noting the characteristics of optical wave propagating in the media. Moreover, the band structure may offer a major reference for studying light transmission and reflection in finite periodic structures [10–13].

One of the major interesting applications of the photonic crystals is the property of omnidirectional reflection, by which lights with some frequency from all of the incident angles are totally reflected for both the TE and TM polarizations [14–16]. As photonic crystals are made of traditional material, omnidirectional reflection is induced by interference of Bragg scattering. However, for the photonic crystal containing metamaterials, omnidirectional reflection may be not induced by Bragg scattering, especially if it occurs in the zero-$\bar{n}$ gap, in which the frequency at center is near the zero average refractive index. The zero-$\bar{n}$ gaps and omnidirectional reflection in the gap of 1D photonic crystals composed of alternative layers of conventional material and metamaterial have been proposed in several studies [10–13,17–20].

Recently, 1D photonic crystals with quasiperiodic structures, especially for Fibonacci sequence, have received a great deal of interest [21–23]. Light transmission and reflection from Fibonacci photonic crystals differ from binary ones. Moreover, omnidirectional reflection and band gaps of Fibonacci photonic crystals containing traditional or metamaterials with frequency independent refractive index have been researched [24–27]. According to measured data from the experiment, the electric permittivity and magnetic permeability of metamaterials are usually frequency dependent [1–9]. Use of frequency independent parameters, the band gaps and omnidirectional reflection of Fibonacci photonic crystals have been presented [28,29]. Most of the studies address the effect induced by different generation orders for a set of a widths of traditional and metamaterial layers and a refractive index of a traditional layer. However, these optical properties are dependent not only on the generation order but also on the width and materials in the structure. In fact, we will present in the paper that zero-$\bar{n}$ gaps are more significantly affected by layer widths and materials than by different generation orders. To the best of our knowledge, the effects of layer widths and materials on zero-$\bar{n}$ gaps and omnidirectional reflection for TE and TM polarizations in Fibonacci basis photonic crystal containing frequency dependent metamaterial have rarely been proposed.

The band structure of 1D photonic crystals can be determined by the dispersion equation, which is formulated by the determinant of the system. For the case with binary basis, the dispersion relation can expressed by the analytical expression, which has been applied to photonic crystals containing conventional material or metamaterial [10–13,17]. However, for the complex basis systems, such as the Fibonacci basis with generation greater than three, since analytical and closed forms of the dispersion relation becomes complex and difficult to formulate, the problem has commonly been explored by numerical methods, including the matrix method. However, in this study, we show that use of the traditional method to find the band gaps and the band structure leads to a numerical instability problem.

In the paper, band structure and band gaps in one-dimensional photonic crystals with a Fibonacci basis con-

*hsuehwj@ntu.edu.tw

taining traditional material and frequency dependent metamaterial are investigated. The band structure is calculated by a band-edge equation, which is derived by topology theory based on a graph model of electromagnetic waves propagating in the photonic crystal. Topology theory with a graph model has been applied to solving networks and some special systems [30–32], but use of the method to solve the band gaps and band structure in planar photonic crystals containing metamaterials has not been proposed. Comparing the present method and the traditional method for the numerical stability of band structure calculation of the planar photonic crystal containing metamaterials is studied. Moreover, omnidirectional zero-$\bar{n}$ gaps in the Fibonacci photonic crystals are investigated not only for different generation orders but also for various widths of each layer and refractive index of the traditional layer.

II. FORMULATION AND THEORY

We consider a one-dimensional periodic photonic crystal with the structure in each cell following the Fibonacci sequence with order j, S_j, by a recurrent relation [21–24]

$$S_{j+1} = S_{j-1}S_j \quad \text{for } j \geqslant 1, \tag{1}$$

with S_0=B and S_1=A. Elements A and B are considered as two layers with thickness d_A and d_B, respectively. In this study, layer B is made of traditional material with frequency independent permittivity ε_B and constant permeability μ_B =1. Thus the refractive index n_B is frequency independent. Layer A is made of metamaterial with frequency dependent permittivity and permeability. Based on the proposed numerical analysis and experiments for artificial metamaterials [3–7,11,28,29], layer A is assumed to be isotopic; lossless and frequency dependent permittivity and permeability are given by

$$\varepsilon_A(\omega) = a_e - \frac{\omega_e^2}{\omega^2}, \tag{2}$$

$$\mu_A(\omega) = a_p - \frac{\omega_p^2}{\omega^2}, \tag{3}$$

where ω is the operation frequency with unit of GHz. ω_e and ω_m are, respectively, the electronic and magnetic plasma frequencies, both of which are considered as 10 GHz in the study.

Let us assume both of materials to be optical isotropic. The electromagnetic waves with TE and TM polarizations propagating in the structure are uncoupled. Thus, the electromagnetic fields, including electric and magnetic fields, with each polarization can be examined separately. For the TE polarization, the electric fields propagating in the photonic crystals are governed by Maxwell's equations. In the jth layer of a cell, the electric field, $\hat{E}(j,x,y,z)$, can be described by

$$\hat{E}(j,x,y,z) = \hat{y}E_y(j,x)\exp(i\omega t - i\beta z), \tag{4}$$

where E_y is the amplitude of the electric field, $\hat{y}$ is the unit vector in the y direction, β is the propagation constant. Since

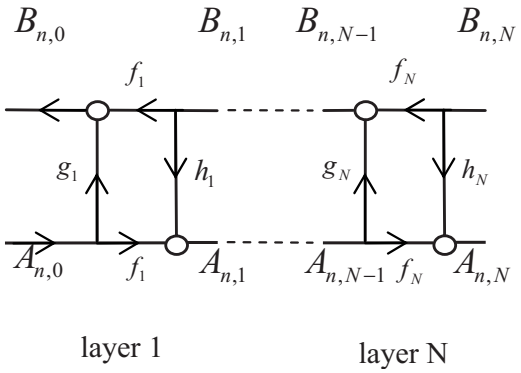

FIG. 1. Graph model for a cell of the Fibonacci photonic crystals.

the medium within each layer is homogeneous and isotropic, the amplitude of the electric field is governed by the wave equation and expressed by summation of forward and backward traveling waves as

$$E_y(j,x) = a_j \exp[-ik_j(x - x_{j-1})] + b_j \exp[ik_j(x - x_{j-1})], \tag{5}$$

where k_j represent the wave vectors, $\pm(k_o^2\varepsilon_j\mu_j - \beta^2)^{1/2}$. ε_j and μ_j are, respectively, the relative permittivity and relative permeability of the media in layer j. According to Maxwell's curl equations, $\nabla \times \hat{E} = -j\omega\mu_j\hat{H}$, the magnetic field in the layer can be expressed by $\hat{H}(j,x,y,z) = [\hat{z}H_z(j,x) + \hat{x}H_x(j,x)]\exp(i\omega t - i\beta z)$, in which the magnetic tangential field H_z is

$$H_z(j,x) = \frac{k_j}{\omega\mu_j}\{a_j \exp[-ik_j(x - x_{j-1})] - b_j \exp[ik_j(x - x_{j-1})]\}. \tag{6}$$

The parameters a_j and b_j can be represented by the electric and magnetic tangential fields at the boundary of the layer according to Eqs. (4) and (5). Thus, we can express the relations between the electric and the magnetic tangential fields at the boundary of the layer as [30,31]

$$E_j = f_j E_{j-1} + h_j \bar{H}_j, \tag{7}$$

$$\bar{H}_{j-1} = f_j \bar{H}_j + g_j E_{j-1}, \tag{8}$$

where $f_j = \sec k_j d_j$, $g_j = (k_j d_1/\mu_j)\tan k_j d_j$, $h_j = (\mu_j/k_j d_1)\tan k_j d_j$, $E_j = E_y(j,x_j)$ and $\bar{H}_j = -i\omega d_1 H_z(j,x_j)$. From Eqs. (7) and (8), we can depict the relations of the amplitudes of the electric and the magnetic tangential fields at the boundary of the layer by a two-way graph model. According to the continuity of the tangential fields in the interface of layers, we can construct the graph model for the cell as shown in Fig. 1.

By topology method, the relations of the amplitudes at the boundary of the cell layer can be expressed by

$$E_N = fE_0 + h\bar{H}_N, \tag{9}$$

$$\bar{H}_0 = f\bar{H}_N + gE_0, \tag{10}$$

where $f=\Pi_{j=1}^{N} f_j / S^{1,N}$, $g=\frac{1}{S^{1,N}}\Sigma_{p=1}^{N} S^{p,N} g_p \Pi_{j=1}^{p-1} f_j^2$, $h=\frac{1}{S^{1,N}}\Sigma_{p=1}^{N} S^{1,p} h_p \Pi_{j=p+1}^{N} f_j^2$. $S^{p,q}$ is the determinant of a part of the graph model for the structure from layers p to q given by [30,31]

$$S^{p,q} = \sum_{s=0}^{q-p} \sum_{i_{2s}=p+s}^{q} \sum_{i_{2s-1}=p+s-1}^{i_{2s}-1} \sum_{i_{2s-1}=p+s-1}^{i_{2s-1}} \sum_{i_{2s-2}=p+s-2}^{i_{2s-1}-1} \cdots \times \sum_{i_2=p+1}^{i_3} \sum_{i_1=p}^{i_2-1} \prod_{u=1}^{s} (-L_{i_{2u-1},i_{2u}}), \tag{11}$$

where $L_{p,q}=h_p g_q \Pi_{j=p}^{q} f_j^2$.

Since wave function propagating in an infinite periodic structure must obey the Bloch waves, the relations between the amplitudes of the electric and the magnetic tangential fields at the ends of a cell are expressed by $E_N = E_0 \exp(iqD)$ and $\bar{H}_N = \bar{H}_0 \exp(iqD)$, where D is the thickness of the basis and q is the Bloch wave vector. Substituting the relations into Eqs. (9) and (10) yields

$$f^2 - 2f\cos(qD) - gh + 1 = 0. \tag{12}$$

As the magnitude of the cosine of the Bloch phase is greater than 1, the Bloch wave is evanescent. The region corresponding to the evanescent wave is called the forbidden gap. If the cosine of Bloch phase is less than 1, the Bloch wave is allowed to propagate through the structure. The region corresponding to the allowed wave is called the allowed band. Thus, the band structure and band gaps that can be determined by the edges of the forbidden gaps, which occurred in the condition of $\cos(qD)=1$ or -1. Here, we define a function Γ_v as $\Gamma_v = f^2 - 2vf + 1 - gh$. The edges of band gaps are satisfied by

$$\Gamma_v = 0, \tag{13}$$

where $v=1$ and -1. The center of the allowed minibands corresponds to $v=0$, which can be used to check the region for the allowed bands and the forbidden gap.

Equation (13) is called the band-edge equation, which is the major equation of this paper. Using the band-edge equation, it is not required to find the band structure and band edges by calculating the cosine of Bloch phase, which is usually used in traditional methods. Unfortunately, calculating the cosine of the Bloch phase may have numerical overflow, especially for the range including the zero-$\bar{n}$ gap as presented in a numerical example in the following section. However, using the present method to find the band structure and band gaps does not have the problem of numerical instability.

For TM polarizations, the dispersion equation can be derived using the same procedures for TE polarizations. If we define $H_y(j,x_j)$ and $i\omega d_1 E_z(j,x_j)$ for layer j as variables H_j and $\bar{E}_j$, respectively, the dispersion equation for TM eigenmodes can be represented by the same form as the TE ones, in which the variables E_j and $\bar{H}_j$ are replaced by the variables H_j and $\bar{E}_j$. Moreover, the parameters f_j, g_j, and h_j are redefined by $\sec k_j d_j$, $k_j d_1 \tan k_j d_j / \varepsilon_j$, and $(\varepsilon_j \tan k_j d_j)/k_j d_1$, respectively. Note, each of the parameters f_j, g_j, and h_j for both TE and TM polarizations does not change as either positive or negative signs for k_j are selected. In other words, both the positive and negative signs for k_j are acceptable for the band gap and band structure analysis by the present method.

III. APPLICATIONS AND DISCUSSIONS OF THE RESULTS

In this section, the band gaps and band structure of the photonic crystal with a Fibonacci basis for TE and TM polarizations are calculated by the present method. The zero-$\bar{n}$ gap and omnidirectional reflection for the photonic crystal are examined. Based on the previous studies [3–7,11], a_e and a_m are chosen by 1.21 and 1.00 in the following examples. It is of special interest in the condition of negative values of both ε_A and μ_A, which are with the operation frequencies in the region of $\omega < \omega_e/\sqrt{a_e}$ and $\omega < \omega_p/\sqrt{a_p}$.

First, we consider a case of photonic crystal with an S_4 basis, by which the structure of the basis is *ABAAB*. The band structure in the photonic crystal with $\varepsilon_B=4$, $d_A=12$ mm $d_B=24$ mm is calculated by the present method and shown in Fig. 2(a), in which the right and left hand sides are for the TE and TM polarizations, respectively. Note that the permittivity and permeability of layer A are zero at the reduced frequencies, $\Omega=0.190$ and $\Omega=0.173$, in which $\Omega=\omega D/(2\pi c)$ and $k_\parallel = \beta D/(2\pi)$ are dimensionless. The reduced frequency corresponding to the zero average refractive index is $\Omega=0.0978$. Near the frequency corresponding to zero of the average refractive index, there is a significant band gap, called the zero-$\bar{n}$ gap. If the photonic crystal is used as a reflector for a light incident from vacuum, the band structure within the light cone corresponds to the reflection of light with a different incident angle. The band structure for $k_\parallel=0$, the center of the light cone, corresponds to the reflection of light incident with 0 deg from vacuum. For $k_\parallel=0$, the zero-$\bar{n}$ gap in the structure is in the range of $\Omega=0.0786-0.1217$. In the figure, the gap in the light cone will differ for different incident angles. As the incident angle of light increases from 0 to 90 deg, the center of the gap almost remains at the same frequency for both the TE and TM polarizations. The edges of light cones, as shown by dotted lines in the figure, for the TE and TM polarizations present the light line of vacuum, corresponding to a 90 deg incident angle from vacuum. The bandgap at the light line of vacuum for the TE and TM polarizations are in the range of $\Omega=0.0844-0.1222$ and $\Omega=0.0788-0.1158$. We find that the bandgap for all incident angles is identical to the overlap of the gap at $k_\parallel=0$ and that at the light line for the TE and TM polarizations. As shown in the gray region of the figure, the omnidirectional reflection of light from the vacuum for the zero-$\bar{n}$ gap exists in the range of $\Omega=0.0844-0.1158$. The phenomenon of the existence of an additional band gap lower than the Bragg gaps may also occur in acoustic waves for phononic crystals or superlattices [33,34].

In Fig. 2(a), we also find a band gap located in the range for positive values of both permittivity and permeability of layer A, called the Bragg gaps, which have been commonly noted in conventional photonic crystals. The gap shifts up in frequency as the incident angle increases from 0 to 90 deg.

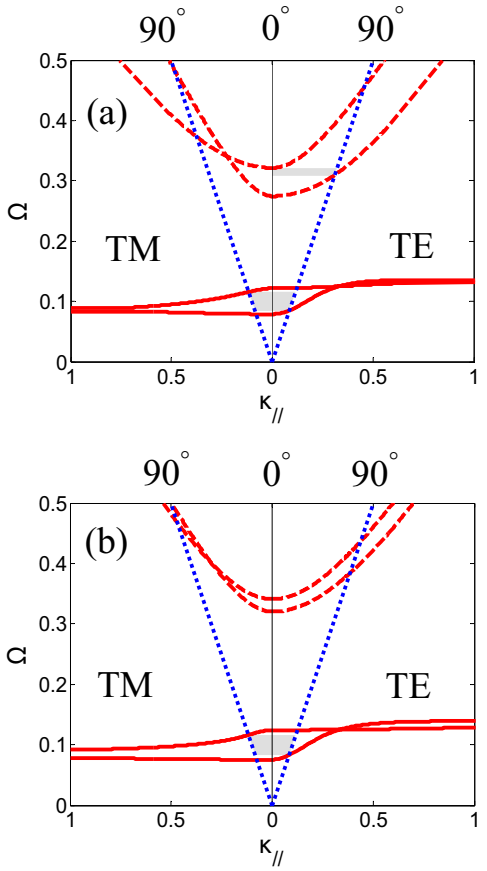

FIG. 2. (Color online) Bragg and zero-$\bar{n}$ gaps of the photonic crystal with S_4 Fibonacci basis. The solid and dashed lines mark the edge of the zero-$\bar{n}$ and Bragg gaps, respectively. The parameters of the photonic crystals are (a) $\varepsilon_B=4$, $d_A=12$ mm, $d_B=24$ mm; (b) $\varepsilon_B=4$, $d_A:d_B=1:2$, $D=36$ mm. The dotted line corresponds to the light lines of the vacuum. The lower gray region marks the omnidirectional reflection from the vacuum. The upper gray region in (a) corresponds to the unidirectional reflection for TE polarization.

For the TM polarizations, a Brewster point may occur in the Bragg gap of the higher incident angle. As seen in the upper gray region of Fig. 2(a), the Bragg gap with center frequency $\Omega=0.315$ has unidirectional reflection of light from the vacuum for TE polarization. As the parameters of the photonic crystal is changed to $\varepsilon_B=4$, $d_A:d_B=1:2$, and $D=36$ mm, the band structure is shown in Fig. 2(b). It is interesting that the Bragg gap vanishes but the zero-$\bar{n}$ gap remains in almost the same location and region.

The band gaps and band structure shown in the figure are determined by the present method, which uses the band-edge equations and band center equation as given in Eq. (13) with $v=1$ and -1 rather than the function $\cos(qD)$ used in traditional methods. The band gap is the region between two band edges, both of which simultaneously correspond to one of $\Gamma_1=0$ and $\Gamma_{-1}=0$. If the calculation range of frequency for the band structure is selected as $0<\Omega<0.5$, we plot the maximum absolute value of Γ_1, Γ_{-1}, and Γ_0 and that of $\cos(qD)$ versus the range of $k_\parallel$ as shown in Fig. 3. We see that the maximum absolute values of Γ_1, Γ_{-1}, and Γ_0, used in this method, almost have the same order for different values of $k_\parallel$. However, the maximum absolute value of $\cos(qD)$ used in the traditional method is increased exponentially as the value of $k_\parallel$ is increased.

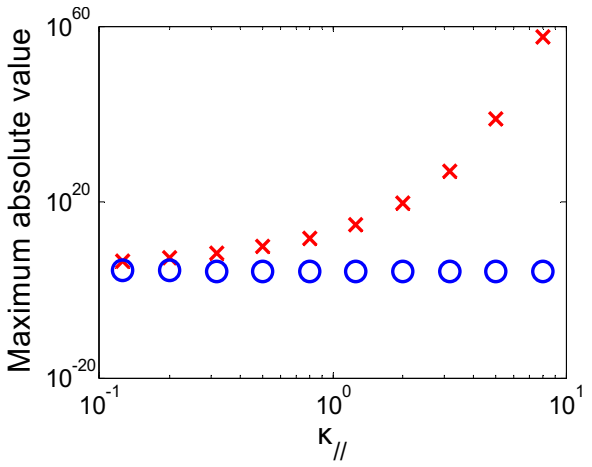

FIG. 3. (Color online) The maximum absolute values in the calculation of zero-$\bar{n}$ gap and band structure by the present method and the traditional methods. The region in $0<\Omega<0.5$ and $0k_\parallel<k_{\parallel,R}$ for the photonic crystal with S_4 Fibonacci basis is considered in the calculation. Γ_1, Γ_{-1}, and Γ_0 are used in the calculation by the present method, but $\cos(qD)$ is used by the traditional methods.

It is interesting to see the effect of the filling factor of layer A (metamaterial), defined by $F=d_A/(d_A+d_B)$, on the omnigap of vacuum near zero $\bar{n}$ in the photonic structure. Let us consider the photonic crystal with S_4 basis as studied in the first case with a different filling factor. Figure 4 present the edges of zero-$\bar{n}$ gap for $k_\parallel=0$ and incident angle 90 deg in the TE and TM polarizations, respectively, by solid, dotted, and dashed lines, versus a different filling factor for layer A. We find the width and the center frequency of the

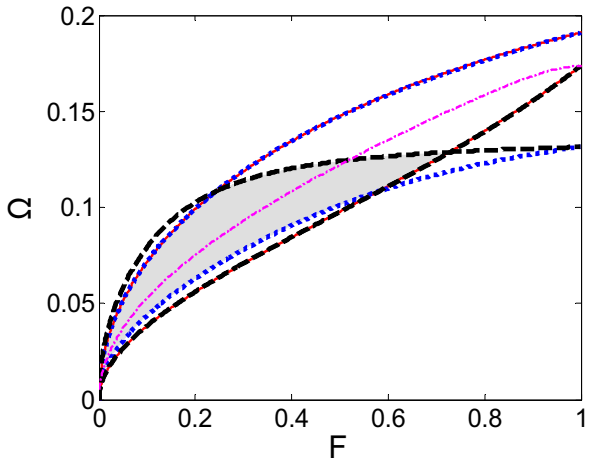

FIG. 4. (Color online) Zero-$\bar{n}$ gap for TE and TM polarizations in the S_4 Fibonacci basis photonic crystal versus the filling factor F of the metamaterials, $F=d_A/(d_A+d_B)$. The dotted, dashed, and solid lines mark the edges of the zero-$\bar{n}$ gap, respectively, crossing the light line of vacuum for TE polarization, light line of vacuum for TM polarization, and perpendicular incident, $k_\parallel=0$. The dashed-dotted line points out the frequency corresponding to the zero $\bar{n}$. The gray region presents the omnidirectional zero-$\bar{n}$ gap for the incidence from the vacuum.

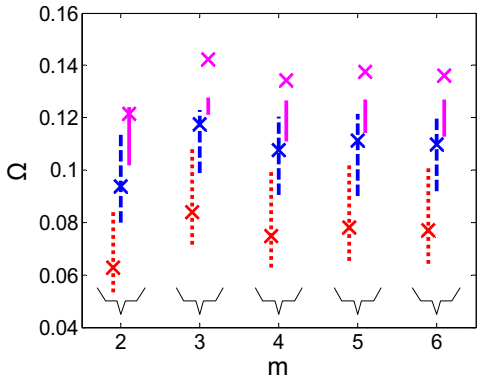

FIG. 5. (Color online) The omnidirectional zero-$\bar{n}$ gap in the S_m Fibonacci basis photonic crystal for the filling factor $F=0.2$, 0.4, and 0.6 versus the generation order m. The dotted, dashed, and solid lines mark the omnigap for the filling factor $F=0.2$, 0.4, and 0.6, respectively. "×" represents the frequency for zero $\bar{n}$. The parameters for the photonic crystals are $\varepsilon_B=4$, $d_A;d_B=1:2$, $D=36$ mm.

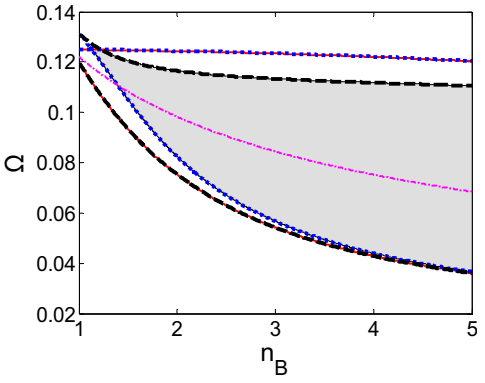

FIG. 6. (Color online) Zero-$\bar{n}$ gap for TE and TM polarizations in the S_4 Fibonacci basis photonic crystal versus refractive index of the layers of traditional material, n_B. The dotted, dashed, and solid lines point to the edges of zero-$\bar{n}$ gap at the edges of the light cone for TE and TM polarization, and the center of the light cone, respectively. The dashed-dotted line marks the frequency corresponding to zero $\bar{n}$. The gray region corresponds to the omnidirectional zero-$\bar{n}$ gap for the incidence from air.

gap are increased from $F=0$ to $F=1.0$ for an incident angle of 90 deg in the TE polarization. However, for an incident angle of 90 deg in the TM polarization, the width of the gap is increased from $F=0$ to $F=0.25$ and decreased from $F=0.25$ to $F=0.73$. The omnigap of the photonic crystals has the maximum value for the filling factor $F=0.25$ and with zero for F greater than 0.73. It is interesting to note the frequencies of zero $\bar{n}$ do not locate within the omnigap if the filling factor of layer A is greater than 0.52.

As the basis of the photonic crystal is replaced by the Fibonacci sequence with a different generation, the omnigap versus the generation order is shown in Fig. 5. We see that the frequencies corresponding to $\bar{n}=0$ for the different Fibonacci basis with $F<0.4$ are almost within the omnigaps and near the center of the omnigaps. The omnigaps in the photonic crystal with different Fibonacci basis have almost the same range for $m>3$. However, these results are quite different from the ones in traditional photonic crystals. If the metamaterial of the photonic crystal are replaced by traditional material with a positive refractive index, the omnigaps may occur in the Fibonacci basis system. However, the omnigaps will have different ranges for a different generation order of the Fibonacci basis in the traditional photonic crystal.

We turn our attention to the effect of the refractive index of material B on the region of the zero-$\bar{n}$ gap. Figure 6 shows the zero-$\bar{n}$ gap in the photonic crystal versus the refractive index of layer B, n_B, from 1.0 to 5.0 for the photonic crystal with S_4 basis, in which $\mu_B=1$, $d_A:d_B=1:2$, $D=36$ mm. We find that the zero-$\bar{n}$ gap vanishes if n_B is less than 1.10. The zero-$\bar{n}$ gap is gradually enlarged as the value of n_B increases. Moreover, the center of the zero-$\bar{n}$ gap is decreased for increasing n_B. The greatest omnigap is from $\Omega=0.037$ to $\Omega=0.111$, occurring at $n_B=5.0$. It is interesting that as n_B is less than 1.4, the frequency corresponding to zero $\bar{n}$ is not within the omnigap.

The omnigap for the photonic crystal with $n_B=1.5$, 2.5, 3.5, and 4.5 versus the generation order is shown in Fig. 7. The parameters for the photonic crystal are $\mu_B=1$, $d_A:d_B=1:2$, $D=36$ mm. We also note the omnigaps almost have the same range for the case of $m>3$. These results are different from the ones in traditional photonic crystals. The omnigaps in the Fibonacci basis photonic crystal made of traditional material will have different ranges for a different generation order.

IV. CONCLUSIONS

We have studied the band gaps and band structure of the planar photonic crystal with Fibonacci basis, which consist of conventional materials and frequency dependent metamaterials. In this study, the band gaps are calculated by a band-edge equation rather than a traditional dispersion equation. Compared with traditional methods, we find using the present method in the calculation has no problems of numerical instability, especially in the region near zero $\bar{n}$ for the photonic crystal containing metamaterial. According to the numerical results, the omnidirectional gap in the Fibonacci

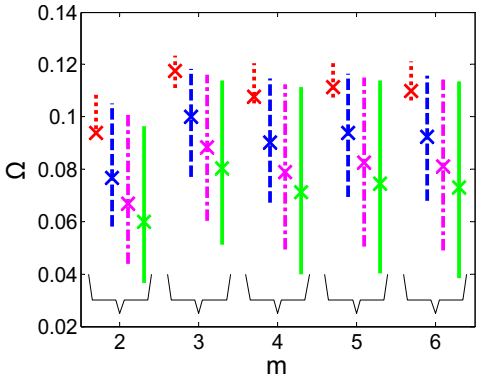

FIG. 7. (Color online) The omnidirectional zero-$\bar{n}$ gap in the S_m Fibonacci basis photonic crystal for $n_B=1.5$, 2.5, 3.5, and 4.5 versus generation order m. The dotted, dashed, dashed-dotted, and solid lines correspond to the omnigap for $n_B=1.5$, 2.5, 3.5, and 4.5, respectively. "×" represents the frequency for zero $\bar{n}$.

basis photonic crystals exists near zero $\bar{n}$. We find that the change in the width and location of the omnidirectional zero-$\bar{n}$ gap is limited when the generation order of the Fibonacci photonic crystals is changed. However, the width of the omnidirectional zero-$\bar{n}$ gap is significantly affected by the filling factor of the metamaterials and approaching a maximum gap for an optimum filling factor. Moreover, as the filling factor is greater than a critical value, the gap becomes zero. For a given metamaterial layer and the filling factor, it is interesting that the gap will be enlarged if the refractive index of the traditional layer is increased.

ACKNOWLEDGMENTS

The authors acknowledge the support in part by the National Science Council of Taiwan under Grant No. NSC 96-2221-E-002-301.

[1] J. B. Pendry, Phys. Rev. Lett. **85**, 3966 (2000).
[2] D. R. Smith, J. Pendry, and M. Wiltshire, Science **305**, 788 (2004).
[3] D. R. Smith and N. Kroll, Phys. Rev. Lett. **85**, 2933 (2000).
[4] R. A. Shelby, D. R. Smith, and S. Schultz, Science **292**, 77 (2001).
[5] J. Pacheco, Jr., T. M. Grzegorczyk, B.-I. Wu, Y. Zhang, and J. A. Kong, Phys. Rev. Lett. **89**, 257401 (2002).
[6] J. Li, L. Zhou, C. T. Chan, and P. Sheng, Phys. Rev. Lett. **90**, 083901 (2003).
[7] T. Koschny, M. Kafesaki, E. N. Economou, and C. M. Soukolis, Phys. Rev. Lett. **93**, 107402 (2004).
[8] A. N. Grigorenko, A. K. Geim, H. F. Gleeson, Y. Zhang, A. A. Firsov, I. Y. Khrushchev, and J. Petrovic, Nature (London) **438**, 335 (2005).
[9] V. M. Shalaev, Nat. Photonics **1**, 41 (2007).
[10] J. A. Monsoriu, R. A. Depine, M. L. Martínez-Ricci, and E. Silvestre, Opt. Express **14**, 12958 (2006).
[11] Y. Xiang, X. Dai, S. Wen, and D. Fan, Phys. Rev. E **76**, 056604 (2007).
[12] N. C. Panoiu, R. M. Osgood, Jr., S. Zhang, and S. R. J. Brueck, J. Opt. Soc. Am. B **23**, 506 (2006).
[13] I. S. Nefedov and S. A. Tretyakov, Phys. Rev. E **66**, 036611 (2002).
[14] E. Yablonovitch, Phys. Rev. Lett. **58**, 2059 (1987).
[15] S. John, Phys. Rev. Lett. **58**, 2486 (1987).
[16] Y. Fink, J. Winn, S. Fan, C. Chen, J. Michel, and J. Joannopoulos, Science **282**, 1679 (1998).
[17] D. Bria, B. Djafari-Rouhani, A. Akjouj, L. Dobrzynski, J. P. Vigneron, E. H. El Boudouti, and A. Nougaoui, Phys. Rev. E **69**, 066613 (2004).
[18] S. Feng, J. M. Elson, and P. L. Overfelt, Phys. Rev. B **72**, 085117 (2005).
[19] I. V. Shadrivov, A. A. Sukhorukov, and Y. S. Kivshar, Phys. Rev. Lett. **95**, 193903 (2005).
[20] F. Villa-Villa and J. A. Gaspar-Armenta, J. Opt. Soc. Am. B **23**, 375 (2006).
[21] M. Kohmoto, B. Sutherland, and K. Iguchi, Phys. Rev. Lett. **58**, 2436 (1987).
[22] W. Gellermann, M. Kohmoto, B. Sutherland, and P. C. Taylor, Phys. Rev. Lett. **72**, 633 (1994).
[23] S. Golmohammadi, M. K. Moravvej-Farshi, A. Rostami, and A. Zarifkar, Opt. Express **15**, 10520 (2007).
[24] R. Pelster, V. Gasparian, and G. Nimtz, Phys. Rev. E **55**, 7645 (1997).
[25] A. G. Barriuso, J. J. Monzón, L. L. Sánchez-Soto, and A. Felipe, Opt. Express **13**, 3913 (2005).
[26] K. Ben Abdelaziz, J. Zaghdoudi, M. Kanzari, and B. Rezig, J. Opt. A, Pure Appl. Opt. **7**, 544 (2005).
[27] D. Lusk, I. Abdulhalim, and F. Placido, Opt. Commun. **198**, 273 (2001).
[28] J. Li, D. Zhao, and A. Liu, Phys. Lett. A **332**, 461 (2004).
[29] F. F. de Medeiros, E. L. Albuquerque, and M. S. Vasconcelos, J. Phys.: Condens. Matter **18**, 8737 (2006).
[30] W. J. Hsueh and J. C. Lin, J. Opt. Soc. Am. B **24**, 2249 (2007).
[31] W. J. Hsueh and H. C. Chen, Phys. Rev. E **76**, 057701 (2007).
[32] W. Mayeda, *Graph Theory* (Wiley, New York, 1972).
[33] Y. A. Kosevich and E. S. Syrkin, Phys. Rev. B **43**, 326 (1991).
[34] Z. Liu, X. Zhang, Y. Mao, Y. Y. Zhu, Z. Yang, C. T. Chan, and P. Sheng, Science **289**, 1734 (2000).